WATER RESOURCES RESEARCH, VOL. 34, NO. 1, PAGES 47–54, JANUARY 1998

Modeling and experimental investigation of transient, nonequilibrium mass transfer during steam stripping of a nonaqueous phase liquid in unsaturated porous media

A. G. J. van der Ham
Department of Chemical Engineering, University of Twente, Enschede, Netherlands

H. J. H. Brouwers
Department of Civil Engineering and Management, University of Twente, Enschede, Netherlands

Abstract. The present paper addresses the one-dimensional unsteady process of steam stripping of the unsaturated zone of soils contaminated with nonaqueous phase liquids (NAPLs). First, the volatilization mechanism and the transport by steam are considered, taking the view that nonequilibrium exists between liquid and vapor phases; second, the effect of evaporation on the specific area is taken into account. The governing equations are rendered dimensionless and solved in closed form. For various dimensionless numbers, solutions are presented, showing the role of the prevailing physical phenomena. Experiments have been performed using two sand mixtures with water and NAPL saturations ranging from 24% to 44% and from 3.8% to 9.4%, respectively. The experimental results confirm the applicability of the theoretical model presented. Furthermore, the analysis results in an empirical correlation for the Sherwood number valid for a broad range of Peclet numbers ($2 < Pe < 60$).

1. Introduction

Nonaqueous phase liquids (NAPLs) are among the most ubiquitous soil contaminants. Though most of these liquids are immiscible with water, they have aqueous phase solubilities that substantially exceed drinking water standards. Contamination of the unsaturated zone by NAPLs and their long-term transport to the groundwater has therefore become one of the major environmental problems in most industrialized countries. Hence, lately, considerable effort has been devoted to the cleanup of sites contaminated with NAPLs.

Current remedies mostly take the form of excavation and cleaning or disposal of the contaminated soil. As the procedures are expensive and sometimes even dangerous, in situ techniques are needed. A cheap and efficient way of cleaning up the soil is offered by in situ executed evaporative techniques. Usually air, water, or steam are employed as stripping media. Enhanced and accelerated cleaning is achieved at elevated temperatures. Hence the use of hot media, such as steam and heated air, can be attractive as short cleaning times are often beneficial, for instance, at sites in commercial use.

In order to optimize in situ cleaning, physical models are required which represent an adequate description of the prevailing processes. To the authors' knowledge the first publication on in situ soil cleaning with steam was by *Maas* [1982]. Subsequently, analysis and experiments of the process were presented by *Hilberts* [1986], *Vreeken and Sman* [1988], *Hunt et al.* [1988a, b], *Udell and Stewart* [1990], and *Falta et al.* [1992a, b]. These elaborations assumed constant steam injection rates and steady steam-front velocities. Furthermore, all previous studies assumed local equilibrium between liquid and vapor phases for the contaminant, though it is recognized that in a large number of practical situations this simplification is not accurate. *Yuan and Udell* [1993] developed a nonequilibrium model for the distillation of a free NAPL and derived a mass transfer coefficient. Free NAPL can be encountered, among other situations, if the liquid contaminant concentration exceeds the solubility limit of the water present. For free NAPL the concentration at the liquid-vapor interface is constant (and proportional to the vapor pressure of the pure contaminant). Recently, *Wilkins et al.* [1995] investigated the nonequilibrium evaporation of NAPL into nitrogen. Steady state conditions were assumed, such as a constant specific area, so that the effect of the shrinking surface on mass transfer was neglected. This was allowed as the maximum decrease in contaminant saturation amounted to 10–15%, and hence the specific interface area was not substantially altered.

The present paper addresses the unsteady evaporation of liquid NAPL and the convective transport of contaminant by the steam. To describe the transfer of the contaminant between liquid and vapor phases, a nonequilibrium model is proposed. As the liquid contaminant concentration exceeds the solubility limit, two immiscible liquid phases are present. Hence the temperature at the liquid-vapor interface is determined by the sum of the individual steam and NAPL saturation vapor pressures which equals the imposed total pressure (in analogy with steam distillation). Furthermore, the shrinkage of the specific area available for mass transfer to the steam, due to evaporation of the NAPL droplet, is taken into account. The governing equations permit an analytical solution which illustrates the influence of the dimensionless numbers concerned. Performed experiments are reported, and it is shown that the results confirm the predictions of the theoretical model. Finally, on the basis of the experiments an empirical correlation for the Sherwood number is put forward which is valid for the range $5 < Pe < 60$.

Paper number 97WR02713.
0043-1397/98/97WR-02713$09.00

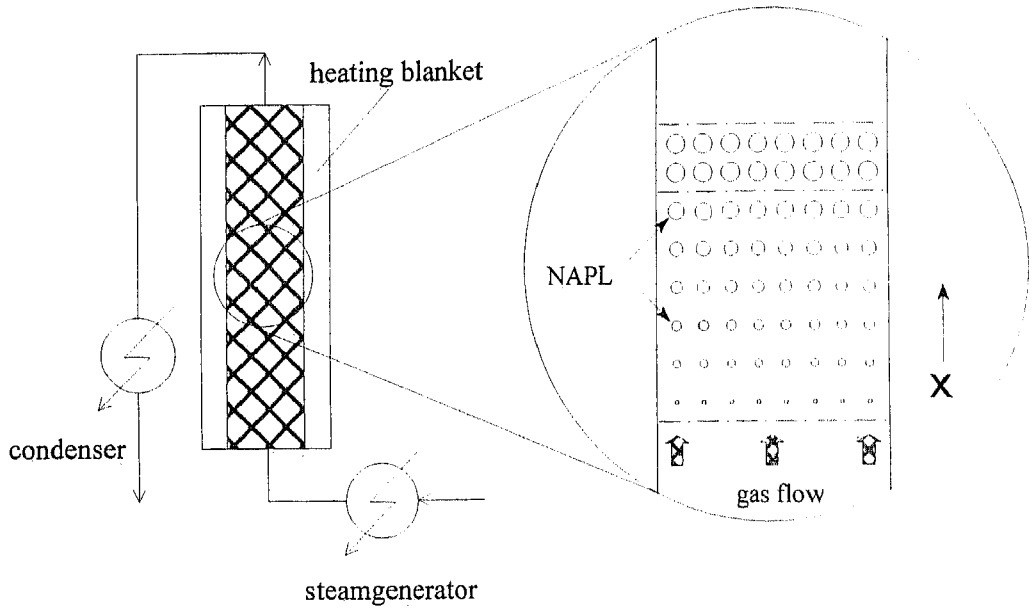

Figure 1. Process representation of steam stripping of nonaqueous phase liquid (NAPL) in a packed bed.

2. Model

The steam stripping process is described in a packed bed of sand, homogeneously contaminated with one single organic component (NAPL), through which steam is flowing. In the bed the NAPL evaporates and is transferred to the steam phase. For a schematic representation of the process, see Figure 1. Start-up phenomena like the heating of the bed up to the operation temperature are neglected here because they take only a minor part of the total cleaning time. Any redistribution of the NAPL due to the heating of the bed up to operation temperature (during start-up) is also neglected.

The fixed bed model is derived from the basic continuity equations for the NAPL component in the vapor phase and in the liquid phase while assuming plug flow behavior for the vapor phase, isothermal operation, and the absence of radial concentration gradients. It is further assumed that the contaminant is homogeneously dispersed as uniform, single-sized bodies throughout the packed bed of sand. During the stripping process the liquid NAPL bodies shrink until they are evaporated. The sand is assumed to be a mixture of nonporous particles with an average diameter $d_{x,50}$. The driving force for the steam stripping process is the difference in the vapor phase NAPL concentration at the liquid interface and in the bulk of the steam flow.

The continuity equation for liquid NAPL in the soil is

$$\phi \frac{\delta S_{p,l}}{\delta t} = k_g a (C_{p,v} - C_{p,i}) \frac{\rho_v}{\rho_{p,l}} \qquad (1)$$

with initial condition

$$S_{p,l}(t = 0,\ 0 \le x \le L) = S_{p,l0}$$

In (1) the porosity ϕ is defined as the fraction of the total bed volume not taken by the sand but by the steam, water, and organic compounds together. The saturation $S_{p,l}$ is the fraction of ϕ taken by the contaminant present as a liquid; k_g is the gas phase mass transfer coefficient; and a is the specific contact area between NAPL and steam. The mole fraction $C_{p,i}$ is the contaminant concentration at the NAPL-steam interf is constant and only a function of temperature fc component. Its value is calculated from vapor press $C_{p,v}$ is the mole fraction of the contaminant in the ste which will be zero at the entrance of the column v clean steam enters. The last term in (1) represents th the molar density of the vapor phase over the liqu phase. $S_{p,l0}$ equals the initial NAPL saturation.

The continuity equation for NAPL in the steam ph

$$\phi S_v \frac{\delta C_{p,v}}{\delta t} + U_v \frac{\delta C_{p,v}}{\delta x} = k_g a (C_{p,i} - C_{p,v})$$

with initial condition

$$C_{p,v}(t = (x\varepsilon)/U_v,\ 0 \le x \le L) = C_{p,i}$$

and boundary condition

$$C_{p,v}(t,\ x = 0) = 0$$

In (2) the saturation S_v is the fraction of the porosit by the vapor phase, and U_v is the superficial vapo The value of S_v is assumed to be constant because tl in $S_{p,l}$ (initial value is typically 0.05) is negligible co S_w, and hence $S_v = S_{v0} = 1 - S_{p,l0} - S_{w,l0}$.

Before solving this set of differential equations transfer parameter $k_g a$ has to be described in m because it depends on the vapor velocity, the spe available for mass transfer, etc. From the studies by *Suzuki* [1966] and *Nelson and Galloway* [1975] it is k the mass transfer coefficient in packed beds at Re described by the general equation (with c_1 a consta the Schmidt number)

$$k_g = c_1 U_v Sc^{-1.5}$$

It shows that the value of k_g is mainly determin packed bed hydrodynamics, which does not chang during the process. In most sand beds the condition 100 is usually fulfilled.

Since k_g is constant, the effect of the shrinking of the NAPL liquid interface on the mass transfer rate $k_g a$ has to be accounted for in the specific droplet area a. Assuming an initial uniform NAPL droplet shape, the specific droplet area a per volume reactor as a function of the NAPL saturation $S_{p,1}$ for various geometries (like cubical or spherical) is given by the following relation:

$$a = a_0\left(\frac{S_{p,1}}{S_{p,10}}\right)^{2/3} \tag{4}$$

with a_0 and $S_{p,10}$ representing the initial specific area and NAPL saturation, respectively. The combination of (3) and (4) results in the following relation for $k_g a$:

$$k_g a = \frac{c_1 U_v}{Sc^{1/3}} a_0\left(\frac{S_{p,1}}{S_{p,10}}\right)^{2/3} = (k_g a)_0\left(\frac{S_{p,1}}{S_{p,10}}\right)^{2/3} \tag{5}$$

with $(k_g a)_0$ being the initial value of $(k_g a)$.

Now Sh_0 and with that $(k_g a)_0$ have been determined by *Wilkins et al.* [1995] as

$$Sh_0 = 10^{-2.79} Pe^{0.62} (d_0)^{1.82} \tag{6}$$

which is valid for $0.05 < Pe < 2$. Rewriting (6) finally yields

$$(k_g a)_0 = 10^{-2.79} u_v^{0.62} D_p^{0.38} d_{s,50}^{-1.38} d_0^{1.82} \tag{7}$$

in which d_0 is the normalized grain size defined as $(d_{s,50}/500\ \mu m)$. Substitution of the independent variable t in (1) and (2) by $t' = t - x/u_v$ yields two almost identical equations:

$$\phi \frac{\partial S_{p,1}}{\partial t'} = -k_g a (C_{p,i} - C_{p,v}) \frac{\overline{\rho_v}}{\rho_{p,1}} \tag{8}$$

$$U_v \frac{\partial C_{p,v}}{\partial x} = k_g a (C_{p,i} - C_{p,v}) \tag{9}$$

Inserting (5) in (8) and (9) and rearranging the resulting equations in dimensionless form yields

$$\frac{\partial \Omega}{\partial \Theta} = -\left(\frac{V_r}{\phi_v}\right)(k_g a)_0 \Omega^{2/3}(1 - Y) \tag{10}$$

$$\frac{\partial Y}{\partial \zeta} = \left(\frac{V_r}{\phi_v}\right)(k_g a)_0 \Omega^{2/3}(1 - Y) \tag{11}$$

for the liquid and vapor phase, respectively, with

$$\Omega(\theta = 0,\ 0 \le \zeta \le 1) = 1 \tag{12}$$

$$Y(\theta > 0,\ \zeta = 0) = 0 \tag{13}$$

as the initial and boundary conditions where Y is the dimensionless contaminant concentration in vapor,

$$Y = \frac{C_{p,v}}{C_{p,i}} \tag{14}$$

Ω is the dimensionless concentration of contaminant in the fixed bed,

$$\Omega = \frac{S_{p,1}}{S_{p,10}} \tag{15}$$

ζ is the dimensionless bed length,

$$\zeta = \frac{x}{L} \tag{16}$$

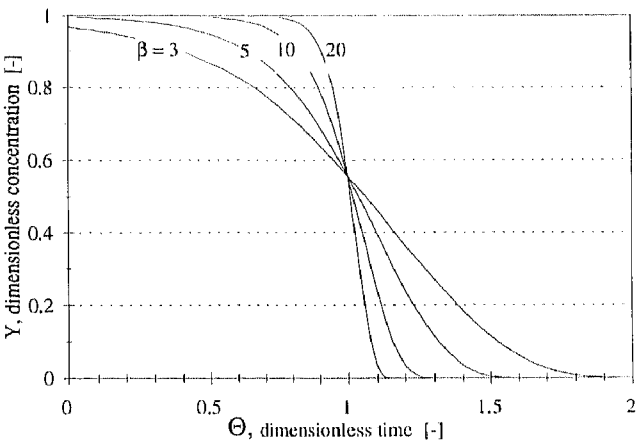

Figure 2. Numerical results for various β values.

Θ is the dimensionless time,

$$\Theta = \frac{t'}{\tau} \tag{17}$$

τ is the minimum time needed for the total removal of the contaminant, i.e., when the outlet concentration is equal to the maximum attainable value for the contaminant concentration (i.e., equals interphase concentration $C_{p,i}$),

$$\tau = \left(\frac{S_{p,10}\phi\overline{\rho_{p,1}}L}{U_v C_{p,i}\overline{\rho_v}}\right) \tag{18}$$

V_r is the reactor volume, AL, and ϕ_v is the volumetric gas flow rate. $U_v A$

The set of two differential equations (equations (10) and (11)) with conditions (12) and (13) is solved analytically according to the method described by *Bischoff* [1969], resulting in an equation for the dimensionless time as a function of the dimensionless concentration Y and the dimensionless location in the column ζ. It is assumed that the "constant pattern" solution (e.g., $Y = \Omega$) is valid, which means that the breakthrough curve is no longer a function of the bed length; that is, it has become constant. The constant pattern solution is valid as long as $\Theta \ge 3/\beta$ and reads

$$\Theta = \zeta + \frac{3}{\beta} - \frac{3}{\beta}\left[\frac{1}{6}\ln(1 - Y) - \frac{1}{2}\ln(1 - Y^{1/3}) + \frac{1}{\sqrt{3}}\arctan\left(\frac{2Y^{1/3} + 1}{\sqrt{3}}\right) - \frac{1}{\sqrt{3}}\arctan\left(\frac{1}{\sqrt{3}}\right)\right] \tag{19}$$

with

$$\beta = \frac{V_r}{\phi_v}(k_g a)_0 = \frac{L}{U_v}(k_g a)_0 \tag{20}$$

The dimensionless number β (usually referred to as the Merkel number or Damköhler number) represents the ratio of the evaporation rate of NAPL over the volumetric flow rate of the steam. Figure 2 shows some typical Y versus Θ curves for different representative values of β. As can be seen, the steepness of the breakthrough curve is a direct function of the β value.

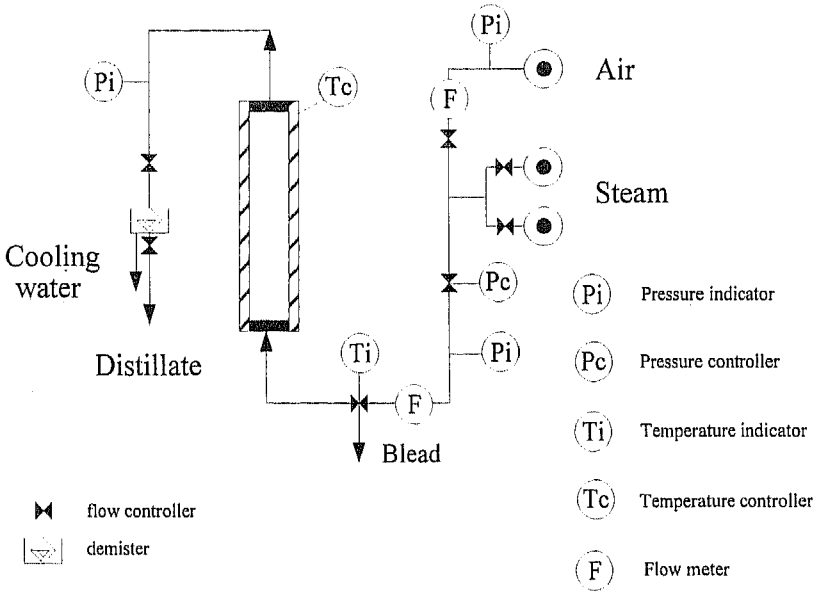

Figure 3. Schematic representation of the test setup.

3. Experimental Study

3.1. Set Up

A setup has been employed that is suited for treating contaminated sand with steam (Figure 3). Basically, the experimental apparatus consisted of (1) a vertically placed pyrex glass tube with an ID of 51 mm (A = 20.43 cm^2), an OD of 56 mm, and a height of 1 m; (2) two steam generators to create a continuous steam supply with a maximum absolute pressure of 4 bar which is reduced to the desired inlet pressure; (3) an electrically heated blanket which is wrapped around the tube to heat up the sand and tube and to avoid heat losses to the surroundings; (4) electrical resistance heating to avoid premature condensation in the supply channels (ID = 0.25 inches); (5) devices to measure pressure, flow, and temperatures; and (6) a condenser to condense water and contaminants.

The sand was mixed with selected amounts of water and contaminant (n-tetradecane) dissolved in acetone and was stirred mechanically. Finally, the acetone was evaporated. Prior to the filling of the column, samples were taken to determine the initial contamination and verify the homogeneity of the sand with respect to the water and contaminant content (samples were also taken after the experiment). The difference between maximum and minimum levels generally amounted to no more than 10%; thus a homogeneous water and contaminant distribution was obtained. Typical dry weight values (dry sand mass divided by wet sand mass) of 90% and n-tetradecane (n-$C_{14}H_{30}$) contamination levels of 10 g kg^{-1} dry weight (dw) were selected. The sand was then poured into the test tube and tamped down. Both ends of the tube were sealed with removable nylon plates with inlet connections and mounted filter screens to prevent the passage of sand and to uniformly disperse fluid flow across the entire cross-sectional area of the column. The porosity of the packed beds ranged from 41% to 46%. The porosity was determined by comparing the bulk density of the packed sand (based on dry matter) and the density of the sand (2650 kg m^{-3}). Two sand mixtures have been employed with their particle size distribution given in Tables 1 and 2, respectively. One can see that the particle distribution of mixture II contains two peaks. For each experiment, new and oven-dried sands were used so that an initial water content of zero was ensured before mixing.

Table 1. Particle Size Distribution of Mixture I

Diameter, μm	Mass Fraction, %
>592	0.00
419–592	1.70
384–419	2.03
352–384	4.47
323–352	8.88
296–323	13.12
271–296	17.73
249–271	18.05
228–249	14.11
209–228	9.95
192–209	5.26
176–192	2.55
161–176	1.20
124–161	0.89
<124	0.00

Here $d_{s,10}$ = 209 μm, $d_{s,50}$ = 264 μm, and $d_{s,90}$ = 345 μm.

Table 2. Particle Size Distribution of Mixture II

Diameter, μm	Mass Fraction, %
>704	0.00
646–704	34.36
592–646	38.53
543–592	13.60
498–543	4.21
419–498	0.61
249–419	0.00
228–249	0.37
209–228	2.22
192–209	2.40
176–192	2.50
161–176	0.86
124–161	0.35
<124	0.00

Here $d_{s,10}$ = 508 μm, $d_{s,50}$ = 625 μm, and $d_{s,90}$ = 683 μm.

Table 3. Initial Conditions Applied at Experiments A, B, C, and D

	A	B	C	D
Sand mixture	I	II	II	II
T_{inlet}, C	105	105	105	112
P_{inlet}, bar	1.2	1.15	1.2	1.5
M, kg	3.05	3.14	3.13	3.13
L, m	0.92	0.92	0.93	0.92
G_v, kg h^{-1}	0.192	0.229	0.307	0.783
$d_{s,50}$, μm	264	625	625	625
ϕ	0.463	0.418	0.413	0.418
$S_{p,10}$	0.038	0.047	0.094	0.092
$S_{w,10}$	0.436	0.297	0.241	0.304
ε	0.244	0.274	0.275	0.252

Here $\varepsilon = (1 - S_{p,10} - S_{w,10})\phi = \phi S_{v,0}$.

Prior to the experiment the column was heated up to a temperature of 100–105°C with the aid of an electric blanket and kept at this temperature for 2–3 hours. During the experiments, steam was injected at the bottom of the column, flushed through the column, and exited at the top into a condenser which was cooled with ice. The steam was injected with an absolute inlet pressure of 1.15–1.5 bar. With a thermometer the steam temperature at the entrance of the tube was measured, showing a slight and negligible superheat of the steam (of the order of 3°C). The condensate flowed to glass bottles where it was collected, sealed, and stored in a refrigerator for analysis. Since the steam flow was constant during an experiment, a fixed filling time was applied, varying from 20 min for experiments A, B, and C to 9 min for experiment D. To avoid volatilization of the contaminant, the condensate was transported from the condenser to the glass bottle by a metal tube. The free contact with ambient air was reduced to a minimum. The contaminant in the condensate samples was extracted with hexane and was analyzed in duplicate by a gas chromatograph equipped with a flame ionization detector. Results yielded the contaminant concentration at the exit versus time.

Laboratory analysis after the experiments revealed that the n-tetradecane concentrations in the lower part of the tube were substantially reduced. This observation was not surprising as the steam was still clean at that location. Higher up in the test column the steam became contaminated with n-tetradecane, and consequently, the driving force for mass transfer between liquid n-tetradecane and steam was less.

3.2. Experimental Results

Four experiments have been conducted, one with mixture I and three with mixture II. In Table 3 and 4 the imposed and the resulting experimental conditions are summarized, respectively. Table 3 shows that the steam flow was smaller during experiment A, for which mixture I was used. This mixture consists of finer sand particles, resulting in a higher flow resistance.

Table 4. Experimental Conditions Applied at Experiments A, B, C, and D

	A	B	C	D
T_{outlet}, K	376.5	375	372.6	377.0
P_{C14H30}, mbar	5.14	4.41	4.14	5.28
$\rho_{p,1}$, kmol m^{-3}	3.57	3.57	3.58	3.56
D_p, m^2 s^{-1}	0.932 10^{-5}	0.925 10^{-5}	0.915 10^{-5}	0.790 10^{-5}
U_v, m s^{-1}	0.0453	0.0542	0.0719	0.186
Pe	5.3	13.4	17.9	58.4
$(k_g a)_{0,Wilkins}$, s^{-1}	0.191	0.288	0.341	0.613
$(k_g a)_{0,fit}$, s^{-1}	0.206	0.248	0.39	1.146

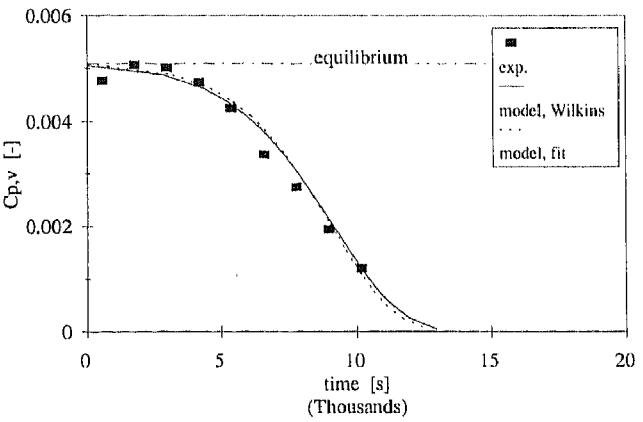

Figure 4. Contaminant mole fraction at exit versus time for experiment A; comparison of experiment and model.

In Figure 4 the mole fraction of n-tetradecane versus time at the exit of the tube is depicted. This fraction is the mean fraction in the steam during the filling time of a sample bottle. In Figures 5–7 the corresponding results of experiments B, C, and D are given.

One can readily see that the n-tetradecane was removed faster during experiment D than during experiment C. During experiment D the inlet pressure was highest, resulting in a higher steam flow and, consequently, in a shorter removal time. A comparison of experiment A and B with experiment D reveals that during the first two experiments the contaminant was removed more slowly. This can be attributed to the much higher vapor velocity during experiment D which enhances the mass transport (see Table 4).

Comparing Figures 5 and 6, which differ in initial contaminant level only, one sees that during experiment C the flushing time corresponding to $C_{p,v} \approx 0.5C_{p,i}$ (or $Y = 0.5$; see (14) and Figure 2) at the exit is about twice as long. As all conditions are practically identical (except $S_{p,10}$) during experiments B and C, Θ for which $Y = 0.5$ and $\zeta = 1$ is equal for

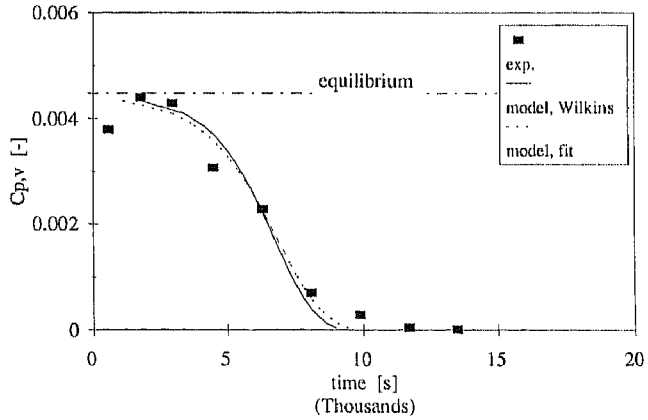

Figure 5. Contaminant mole fraction at exit versus time for experiment B; comparison of experiment and model.

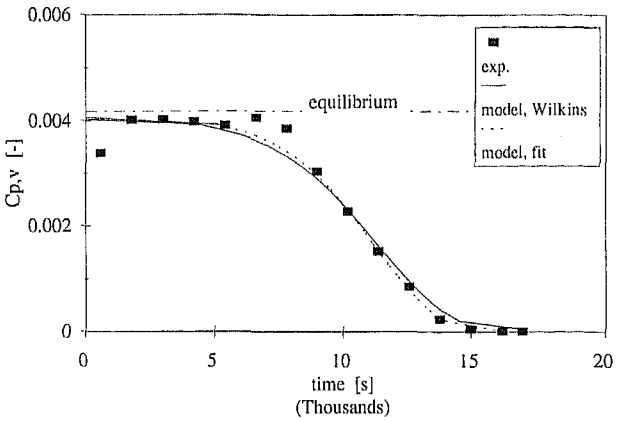

Figure 6. Contaminant mole fraction at exit versus time for experiment C; comparison of experiment and model.

both situations. So, the actual time at which $C_{p,v} \approx 0.5C_{p,i}$ depends linearly on $S_{p,10}$; see (18).

In order to investigate the removal efficiency of *n*-tetradecane, analyses of sand samples were conducted before and after the experiments. These experiments yielded the water content and the contaminant content. In Table 5 the results of these analyses are summarized. The analyses of condensate and sand are used to check the mass balance of water and contaminant, which is summarized in Tables 6 and 7. The "removed amount" is based on soil analysis before and after the experiment while the "stripped amount" is based on condensate analysis. One can see that the relative error varies between 5% and 13%, implying an acceptable accuracy of the applied sampling techniques and the experimental results. The laboratory analyses after the experiments reveal that the *n*-tetradecane concentration in the tubes are substantially reduced (Table 5). The key words bottom and top correspond to the first centimeters of bottom and top sand, respectively.

4. Comparison Model and Experimental Results

In this section the analytical model is tested against the experimental results of the experiments A–D. Values of the necessary model parameters like the physical constants, the reactor dimensions, the operation parameters, and the initial mass transfer rate $(k_g a)_0$, according to *Wilkins et al.* [1995],

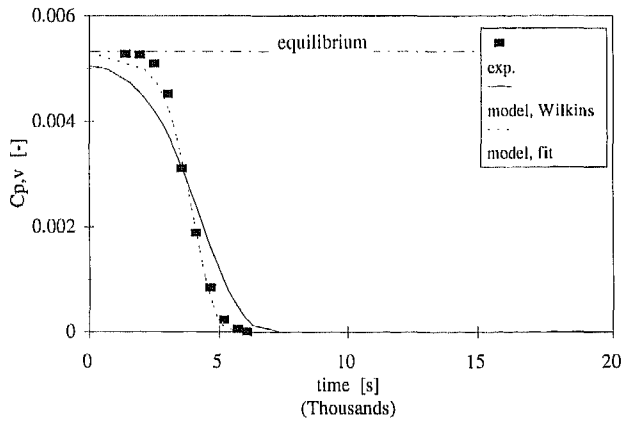

Figure 7. Contaminant mole fraction at exit versus time for experiment D; comparison of experiment and model.

Table 5. Contaminant Concentration in Sand Before and After Experiments in Milligram Contaminant Per Kilogram of Dry Mass

	A	B	C	D
Initial top	8.775	8.293	17.05	17.05
Final top	0.803	1.675	2.24	2.41
Initial bottom	8.775	9.720	18.35	18.35
Final bottom	0.803	1.864	2.29	2.03

Bottom and top correspond to the first centimeters of the bottom and top of the sand column.

are summarized in Table 3 and 4. Correlations applied to calculate the molar density, vapor pressure, and diffusivity of the contaminant are shown in Table 8. Note that (1) the value of the molar fraction of the contaminant in the vapor $(C_{p,i})$ is defined as the ratio of the contaminant partial pressure over the total pressure and (2) the initial contaminant saturation $(S_{p,10})$ is defined as follows:

$$S_{p,10} = \frac{C_{p,s}}{1000} \frac{(1-\phi)}{\phi} \frac{\rho_s}{\rho_{p,l}} \tag{21}$$

where $C_{p,s}$ is the contaminant concentration in the sand on a dry basis (grams of contaminant per kilogram of dry sand) as tabulated in Table 5, ρ_s is the dry sand density specified as 2650 kg m^{-3}, and $\rho_{p,l}$ is the liquid contaminant density.

In Figures 4–7 the model predictions based on the initial mass transfer rate $(k_g a)_0$ value according to *Wilkins et al.* [1995] are depicted as solid lines, and the lines $C_{p,v} = C_{p,i}$ are marked "equilibrium." For the experiments A, B, and C the fit was reasonably good, especially if one takes into account that no fitting parameter was used. On the other hand, the results for experiment D are not that good, the slope of the curve being too flat, implying that the initial $(k_g a)_0$ value was too low.

As an alternative, the $(k_g a)_0$ value was used as a fitting parameter to obtain an optimal curve through the experimental points (see the dashed lines in Figures 4–7). The optimal fitted values of $(k_g a)_0$ obtained are shown in Table 4. Comparison of $(k_g a)_0$ values according to *Wilkins et al.* [1995] with our fitted values shows that for experiment A the values are almost equal and for experiment B and C the values are within 20%, as expected. For experiment D the fitted value is 90% higher.

The correlation of *Wilkins et al.* [1995] is valid for initial conditions and for the range $0.05 < Pe < 2$, which is below the Peclet numbers applied in the experiments reported here (see Table 4). Furthermore, the results show that the difference between $(k_g a)_0$ according to *Wilkins et al.* [1995] and $(k_g a)_{0,\text{fit}}$ increases with increasing Peclet number. It is clear that extrapolation of the $(k_g a)_0$ correlation according to

Table 6. Mass Balance for Water

	A	B	C	D
Supplied amount of steam, g	636	924	1624	1446
Collected amount in condenser, g	606	923	1458	1319
Increased amount in column, g	−54	92	88	43
Difference, g	84	−90	78	85
Relative difference, %	13%	−10%	5%	6%

Table 7. Mass Balance for Contaminants

	A	B	C	D
Initial amount in column, g	23.5	26.2	52.1	51.3
Final amount in column, g	2.2	5.1	6.7	6.4
Removed amount, g	21.3	21.1	45.4	44.9
Stripped amount, g	24.3	18.7	39.6	42.5
Difference, g	−3.0	2.4	5.8	2.4
Relative difference, %	−13%	9%	11%	5%

The units are in grams $C_{14}H_{30}$.
The final amount in the column is measured by analyzing a top and a bottom sample (see Table 5) and multiplying the average value (in grams of NAPL per kilogram of dry solid) with the dry solid content of the column.

Wilkins et al. [1995] will results in an erroneous description of the breakthrough curve.

Correlating the $(k_g a)_{0,\text{fit}}$ results following a correlation similar to that presented by *Wilkins et al.* [1995] and using 1.82 for the power of d_0 results in

$$Sh_0 = 10^{-3.03} Pe^{0.88} d_0^{1.82} \qquad 5 < Pe < 60 \qquad (22)$$

with $r^2 = 0.95$.

Analogous to correlations found in the literature, $d_{s,50}$ is used as the length scale in the Sherwood and Peclet numbers. Comparison with the correlation of *Wilkins et al.* [1995] shows that the power of Pe is increased to 0.88 and that the constant is somewhat smaller. This increased power of Pe is in closer agreement with the correlations proposed by *Kunii and Suzuki* [1966] and *Nelson and Galloway* [1975] which show a power of 1 in Pe. In Figure 8 the experimental data and a line according to (22) are presented graphically, together with the experimental data of *Wilkins et al.* [1995] for $Pe > 1$, provided by M. D. Wilkins (personal communication, 1996). Correlation (22) appears to be in close agreement with all experimental data for $2 < Pe < 60$. For $Pe < 2$ the correlation proposed by *Wilkins et al.* [1995] is recommended.

Table 8. Correlations Used for Calculating Physical Constants of *n*-Tetradecane (*n*-$C_{14}H_{30}$) and Water

Physical Property	Correlation	Method
Molar vapor density, mol m^{-3}	$\rho_v = P_{\text{tot}}/RT$ where P_{tot} is in Pascals, T is in Kelvins; and R = 8,314 J mol^{-1} K^{-1}	ideal gas law
Molar liquid NAPL density, mol m^{-3}	$\rho_{p,l} = A/B^{(1+(1-T/C)^D)}$ where A = 0.304; B = 0.256; C = 692; D = 0.273, and T is in Kelvins	Daubert and Danner
Gas diffusivity of NAPL and steam, m^2 s^{-1}	$D = 3.185 \times 10^{-10} T^{1.75}/P_{\text{tot}}$ where P_{tot} is in bar, and T is in Kelvins	Fuller et al.
Vapor pressure of water and *n*-tetradecane, bar	$\ln P^\circ = A - B/(T + C)$ where for *n*-tetradecane, A = 9.51; B = 4009; and C = −105, and for water, A = 11.66; B = 3816; C = −46.1; and T is in K	Antoine vapor pressure equation

Each method is described by *Reid et al.* [1987] in more detail.

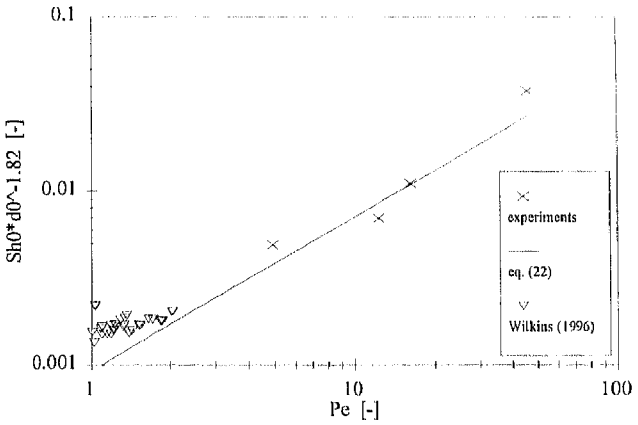

Figure 8. Experimental and theoretical (equation (22)) representation of $Sh_0/d_0^{1.82}$ versus Pe.

5. Conclusions

The volatilization of a nonaqueous phase liquid from a partially water-saturated sand bed was investigated. A conceptual model was derived that accounted for the interphase mass transfer between liquid NAPL blobs and a stripping medium and for the shrinking of the specific surface area (of the blobs) available for mass transfer. The governing partial differential equations were rendered dimensionless and solved in closed form. Solutions of the equations were presented as functions of the main dimensionless parameter, the Merkel/Damköhler number. This number represents the ratio of the maximum evaporation rate of NAPL over the maximum removal flow rate of NAPL by the stripping medium.

Furthermore, one-dimensional bench-scale experiments were reported to validate the model. The *n*-tetradecane was used as NAPL; steam was used as the stripping medium; and the packed bed was composed of one of two sand mixtures. During the experiments ~90% of the initial NAPL was removed, illustrating the true transient character of the process, and a substantial shrinking of the specific area was therewith obtained.

Application of the *Wilkins et al.* [1995] correlation for estimation of the main dimensionless parameter of the model showed reasonably good agreement between the modeled and experimentally obtained breakthrough curve as long as the applied Pe number was low. Unfortunately, the results are poor for experiments conducted at high Pe numbers. This effect is mainly due to the limited applicability of the Wilkins et al. correlation at the experimental conditions applied. On the basis of the experiments a new empirical correlation for Sh_0 was put forward as a function of Pe and d_0 which is applicable for $2 < Pe < 60$ and which is useful for engineering computations concerning stripping of unsaturated sandy soils.

Notation

A cross-sectional area of the column, m^2.
a specific surface area, m^2 m^{-3}.
C_p contaminant molar fraction in vapor phase.
$C_{p,s}$ contaminant mass fraction on the sand.
d_0 normalized grain size ($d_{s,50}/0.05$ cm).
d_s sand diameter, m.
$d_{s,50}$ sand diameter for which 50% of the sand mass is finer, m.

D_p diffusion coefficient of contaminant and stripping medium, $m^2\ s^{-1}$.
G_v mass flow rate of vapor, $kg\ s^{-1}$.
k_g vapor liquid mass transfer coefficient, $m\ s^{-1}$.
L length of packed bed, m.
M amount of contaminated and moistened sand in column, kg.
P pressure, bar.
P° partial pressure, bar.
Pe Peclet number, equal to $u_v d_{s,50}/D_p$, dimensionless.
Re Reynolds number, equal to $U_v d_{s,50}/\nu_v$, dimensionless.
S saturation.
Sc Schmidt number, equal to ν_v/D_p, dimensionless.
Sh Sherwood number, equal to $(k_g a)_0 d_{s,50}^2/D_p$, dimensionless.
t time, s.
T temperature, K.
u interstitial velocity, equal to U/ε, $m\ s^{-1}$.
U superficial velocity, $m\ s^{-1}$.
V_r volume of bed, m^3.
x axial coordinate, m.
Y dimensionless contaminant concentration in vapor phase.

Greek symbols

β Merkel or Damköhler number $(=L(k_g a)_0/U_v)$.
ε effective porosity, approximately equal to $\phi(1 - S_{w,10} - S_{p,10}) = \phi S_{v,0}$.
ζ dimensionless axial coordinate.
Θ dimensionless time.
ν kinematic viscosity, $m^2\ s^{-1}$.
ρ density, $kg\ m^{-3}$.
$\bar{\rho}$ molar density, $mol\ m^{-3}$.
τ time constant, equation (18), s.
ϕ fraction of bed not taken by the sand.
ϕ_v volumetric vapor flow rate, $m^3\ s^{-1}$.
Ω dimensionless contaminant concentration in packed bed.

Subscripts

i interface.
l liquid.
p contaminant.
s sand.
v vapor.
0 initial condition.

Acknowledgments. The authors are indebted to H. Menkehorst and C. C. W. Leemreize, who performed the experimental runs.

References

Bischoff, K. B., General solution of equations representing effects of catalyst deactivation in fixed-bed reactors, *Ind. Eng. Chem. Fundam.*, *8*, 665–668, 1969.

Falta, R. W., K. Pruess, I. Javandel, and P. A. Witherspoon, Numerical modeling of steam injection for the removal of nonaqueous phase liquids from the subsurface, 1, Numerical formulation, *Water Resources Res.*, *28*, 443–449, 1992a.

Falta, R. W., K. Pruess, I. Javandel, and P. A. Witherspoon, Numerical modeling of steam injection for the removal of nonaqueous phase liquids from the subsurface, 2, Code validation and application, *Water Resources Res.*, *28*, 451–465, 1992b.

Hilberts, B., In-situ steam stripping, in *Proceedings of the First International TNO Conference on Contaminated Soil*, edited by J. W. Assink and W. J. van den Brink, pp. 680–686, Martinus Nijhoff, Dordrecht, Netherlands, 1986.

Hunt, J. R., N. Sitar, and K. S. Udell, Nonaqueous phase liquid transport and cleanup, 1, Analysis of mechanisms, *Water Resources Res.*, *24*, 1247–1258, 1988a.

Hunt, J. R., N. Sitar, and K. S. Udell, Nonaqueous phase liquid transport and cleanup, 2, Experimental studies, *Water Resources Res.*, *24*, 1259–1269, 1988b.

Kunii, D., and M. Suzuki, Particle-to-fluid heat and mass transfer in packed beds of fine particles, *Int. J. Heat Mass Transfer*, *10*, 845–852, 1966.

Maas, J. G., Method of cleaning polluted subsoil and apparatus for carrying out the method, *Patent GB 2098644A*, England, United Kingdom, 1982.

Nelson, P. A., and T. R. Galloway, Particle-to-fluid heat and mass transfer in dense systems of fine particles, *Chem. Eng. Sci.*, *30*, 1–6, 1975.

Reid, R. C., J. M. Prausnitz, and B. E. Poling, *The Properties of Gases and Liquids*, 4th ed., McGraw-Hill, New York, 1987.

Udell, K. S., and L. D. Stewart, Combined steam injection and vacuum extraction for aquifer cleanup, in *Subsurface Contamination by Immiscible Fluids*, edited by Weyer, pp. 327–335, Balkema, Rotterdam, Netherlands, 1990.

Vreeken, C., and H. T. Sman, Physical techniques for the in-situ cleaning of contaminated soil, in *Contaminated Soil '88*, edited by K. Wolf, W. J. van den Brink, and F. J. Colon, pp. 891–900, Kluwer Acad., Norwell, Mass., 1988.

Wilkins, M. D., L. M. Abriola, and K. D. Pennell, An experimental investigation of rate-limited nonaqueous phase liquid volatilization in unsaturated porous media: Steady state mass transfer, *Water Resources Res.*, *31*, 2159–2172, 1995.

Yuan, Z. G., and K. S. Udell, Steam distillation of a single component hydrocarbon liquid in porous media, *Int. J. Heat Mass Transfer*, *38*, 1965–1976, 1993.

H. J. H. Brouwers, Department of Civil Engineering and Management, University of Twente, P. O. Box 217, 7500 AE Enschede, Netherlands. (e-mail: h.j.h.brouwers@sms.utwente.nl)

A. G. J. van der Ham, Department of Chemical Engineering, University of Twente, P. O. Box 217, 7500 AE Enschede, Netherlands. (e-mail: a.g.j.vanderham@ct.utwente.nl)

(Received May 24, 1996; revised September 19, 1997; accepted September 24, 1997.)